A miniature laser speckle fluorescence sectioning microscope for cell imaging

Yonghong Shao (邵永红), Heng Li (李 恒), Qiao Wen (文 侨), Yan Wang (王 岩), Junle Qu (屈军乐)*, and Hanben Niu (牛憨笨)

Key Laboratory of Optoelectronic Devices and Systems of Ministry of Education and Guangdong Province, Institute of Optoelectronics, Shenzhen University, Shenzhen 518060, China

**E-mail: jlqu@szu.edu.cn*

Received June 17, 2010

We present a miniature fluorescence sectioning microscope which uses a diode-pumped solid-state (DPSS) laser as the light source and a fast translating diffuser to produce dynamically changing speckle patterns onto the back aperture of the objective to illuminate the sample. Optical sectioning, which originates from the statistical characteristics of laser speckles, is obtained by calculating the contrast of a series of fluorescence images. High contrast fluorescence sectioning images of bovine pulmonary artery endothelial (BPAE) cells are obtained. The image quality is similar to that of the images acquired by standard laser scanning confocal microscope (LSCM). Compared with LSCM, the laser speckle fluorescence microscope (LSFM) presented in this letter has many advantages, such as simple configurations, low cost, compact, and easy to operate, which makes it possible to have wide spread applications in biomedicine.

OCIS codes: 170.1790, 180.1790, 180.2520, 180.6900.

doi: 10.3788/COL20100810.0944.

Cells are basic units of structure and function in organism. The mechanics of cells are closely related to their organic components. The cytoskeleton, a cellular "scaffolding" or "skeleton" contained within the cytoplasm, is made out of proteins. It is a dynamic structure that maintains cell shape, protects the cell, enables cellular motion (using structures such as flagella, cilia, and lamellipodia), and plays important roles in both intracellular transport (e.g., the movement of vesicles and organelles) and cellular division. The change of cellular functions in diseased cells generally leads to the change of cytoskeleton. Mechanical properties of individual living cells are known to be closely related to the health and function of the human body. Therefore, the observation and analysis of the fine structures and the distribution of molecules inside the cells are very important to the study of biological phenomena in cells[1,2].

Laser scanning confocal microscopy (LSCM) has unique optical sectioning capability, which allows for the observation and analysis of three-dimensional (3D) structures of cells non-invasively. LSCM has become a widely used tool in the study of cellular morphology, dynamic 3D imaging, and 3D reconstruction of cells[3−10]. In LSCM, a confocal pinhole is used to eliminate the fluorescence light from outside of the focal plane, and a single focused light spot is scanned across the sample by scanning mirrors, which would require a complex configuration of LSCM, implying that the optics is hard to align and the system is expensive and not straightforward to operate.

Compared with LSCM, standard wide-field fluorescence microscopy is relatively inexpensive and convenient to use for its simple configuration and the matured technology. Therefore, it has become an indispensible tool in biomedicine. However, a wide-field fluorescence microscopy does not have optical sectioning capability. In addition, the image contrast is poor because the light from the focal plane as well as from below and above the focal plane reaches the detector, such as a charge-coupled device (CCD) camera. Optical sectioning has been demonstrated by implementing structured illumination[11−14] and dynamic speckle illumination[15,16] in a wide-filed fluorescence microscope. We have previously developed a wide-field fluorescence sectioning microscope using speckle illumination in imaging thick samples[17]. Dynamic speckle patterns are produced by a fast translating diffuser for illuminating the sample, and a series of fluorescence images are acquired with a CCD camera. Optical sectioning is obtained from the illumination pattern statistics. This technique has been successfully used in optical sectioning of tissues[18]. In this letter, we report the development of a miniature laser speckle fluorescence microscope (LSFM) that uses a small diode-pumped solid-state (DPSS) laser and has sectioning capability similar to a confocal microscope. High contrast fluorescence sectioning images of bovine pulmonary artery endothelial (BPAE) cells are obtained with the setup, demonstrating its potentials in cell imaging.

The schematic of the miniature LSFM is shown in Fig. 1. A DPSS laser is implemented in a standard wide-field fluorescence microscope (Leica DMLB2). The output wavelength of the laser is 473 nm. A diffuser, which is mounted on a translating motor, is inserted into the optical path. In this setup, granule size and transmission of the diffuser are 120 and 70%, respectively. Generally, the lateral resolution is determined by the equation $d = 1.22\lambda f/D$, where λ is the wavelength, f is the focal length of the lens, and D is the spot size. In order to obtain high spatial resolution, the back aperture of the objective should be fully illuminated. The output of the laser is expanded to a beam of about 2.5 mm in diameter and then collimated before being incident on the diffuser. The illuminated area of the diffuser is amplified three times by lenses and then projected onto the back aperture of the objective (40×, (NA) 0.65) to illuminate the sample by speckle patterns. Dynamically changing

speckle patterns are produced by translating the diffuser using the step motor. A series of fluorescence images of the sample are then acquired with a CCD camera, which are then processed to reconstruct the sectioning image of the sample using the following statistical image processing algorithms[15]:

$$I_{\mathrm{RMS}} = \left\{ [\sum_{i=1}^{N} (I_i - I_{i-1})^2)]/2N \right\}^{1/2}, \qquad (1)$$

where I_{RMS} is the root mean square of the series of acquired images and is proportional to the fluorescence intensity, N is the number of acquired images, i is the image serial number, and I_i is the intensity of the ith image. N is approximately 40−60.

In order to demonstrate the sectioning capability of the miniature LSFM, and particularly its application in cell imaging, we performed fluorescence sectioning imaging of BPAE cells. The cells were stained with red-fluorescent Texas Red-X phalloidin for labeling F-actin and with mouse monoclonal anti-α-tubulin in conjunction with green-fluorescent BODIPYFL goat anti-mouse IgG for labeling microtubules and blue-fluorescent DAPI for labeling the nuclei. The laser power on the sample was approximately 5 mW, and the exposure time of the CCD camera was 100 ms. The step size of the motor was 50 μm. A series of fluorescence images were acquired for reconstructing the sectioning image at the focal plane.

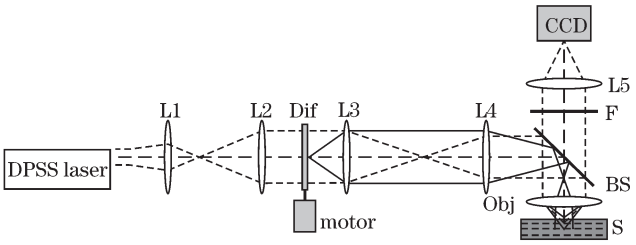

Fig. 1. Schematic diagram of the miniature laser speckle fluorescence sectioning microscope. L1−L5: lens; Dif: glass ground diffuser; Obj: objective; BS: dichroic beam splitter; F: filter; S: sample.

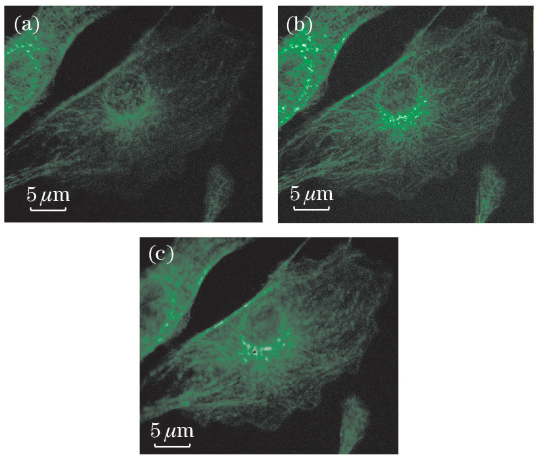

Fig. 2. Fluorescence sectioning of BPAE cells at different depths d inside the cell slide. (a) $d = 0$, (b) $d = 2$ μm, and (c) $d = 4$ μm.

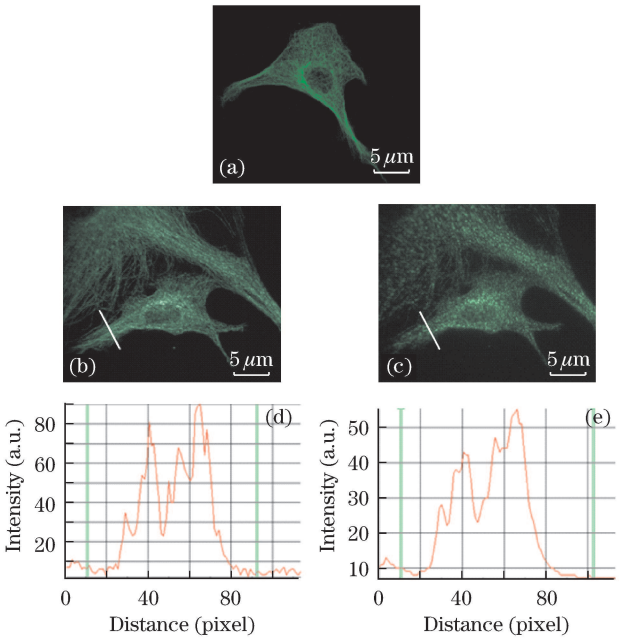

Fig. 3. Comparison of imaging performance of the miniature LSFM with that of LSCM and wide-field fluorescence microscope. (a)−(c) Fluorescence images of BPAE cells obtained using (a) LSCM, (b) miniature LSFM, and (c) wide-field fluorescence microscope. (d) and (e) are the intensity profiles along the lines in images (b) and (c).

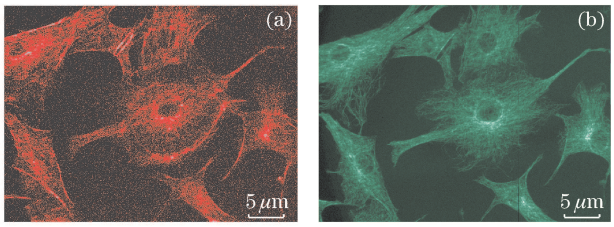

Fig. 4. Fluorescence images of BPAE cells (a) at 520 nm and (b) 620 nm. The images show the distribution of (a) F-actin and (b) microtubules in the cells.

The sample stage was moved along the z axis at the step size of 2 μm so that fluorescence images of BPAE cells at different depths were obtained. Fluorescence images in Fig. 2 clearly show the microtubules.

We then compared the imaging performance of the miniature LSFM with that of confocal microscope and standard wide-field fluorescence microscope. Figure 3 shows the images of the same stained BPAE cells obtained using confocal microscope, the miniature LSFM, and a wide-field fluorescence microscope. Figure 3(b) clearly shows the structure of microtubules, which is similar to the image obtained using a LSCM (Fig. 3(a)), and sharper than the image obtained using wide-field fluorescence microscope (Fig. 3(c)). Figures 3(d) and (e) are the fluorescence intensity profiles along the lines in Figs. 3 (b) and (c), respectively, which show that the image Fig. 3(b) has a higher contrast than Fig. 3(c) does.

Two narrow band pass filters (520±13 and 620±13 nm) were inserted into the optical path of the LSFM system and a series of images were acquired. These images were then used to reconstruct the depth sectioning images of BAPE cells at two different emission wavelengths. As

shown in Fig. 4(a), F-actin, which is corresponding to the 520-nm channel, mainly distributes near the cell membrane and nuclear membrane area. Figure 4(b) clearly shows the distribution of microtubules.

In conclusion, we focus on the development of a miniature laser speckle fluorescence sectioning microscope and its application to cell imaging. The system is based on the redesign of a standard wide-field fluorescence microscope. We use a 473-nm DPSS laser as the light source which by illuminating a translating diffuser produces speckle patterns at the back aperture of the microscope objective to illuminate the cells. Fluorescence sectioning is achieved by calculating the contrast of a series of fluorescence images. Experimental results with BPAE cells show that this method provides a low cost and convenient way of obtaining depth sectioning for cell imaging, as well as its capability for multicolor imaging. Compared with LSCM, the wide-field fluorescence sectioning microscope presented in this work can obtain depth-resolved images with similar lateral resolutions and depth discrimination with a compact and cost-effective system, which makes it potentially to be applied widely in biomedicine.

This work was supported by the National Natural Science Foundation of China (No. 60627003) and the Science and Technology Program of Guangdong Province (No. 2008A060205003) and Shenzhen (No. ZYC20090325 0207A).

References

1. S. Woolner, A. L. Miller, and W. M. Bement, Cytoskeleton Methods and Protocols **586,** 23 (2009).
2. G. Paulsen, F. Lauritzen, M. L. Bayer, J. M. Kalhovde, I. Ugelstad, S. G. Owe, J. Hallen, L. H. Bergersen, and T. Raastad, J. Appl. Physiol. **107,** 570 (2009).
3. G. J. Brakenhoff, H. T. M. Vandervoort, E. A. Van Spronsen, W. A. M. Linnnemans, and N. Nanninga, Nature **317,** 748 (1985).
4. J. G. White and W. B. Amos, Nature **328,** 183 (1987).
5. S. W. Paddock, Biotechniques **27,** 992 (1999).
6. R. H. Webb, Rep. Prog. Phys. **59,** 427 (1996).
7. P. Furrer, J. M. Mayer, and R. Gurny, J. Ocular Pharmacology and Therapeutics **13,** 559 (1997).
8. W. B. Amos and J. G. White, Biol. Cell **95,** 335 (2003).
9. Q. Yu, X. Yu, and M. Bi, Acta Opt. Sin. (in Chinese) **29,** 3057 (2009).
10. D. Sha, Q. Jiang, W. Zhao, and L. Qiu, Chinese J. Lasers (in Chinese) **37,** 1157 (2010).
11. M. A. A. Neil, R. Juskaitis, and T. Wilson, Opt. Lett. **22,** 1905 (1997).
12. R. Heintzmann, T. M. Jovin, and C. Cremer, J. Opt. Soc. Am. A **19,** 1599 (2002).
13. G. L. Gustafsson, S. Lin, M. Peter, C. J. Carlton, R. Wang, I. N. Golubovskaya, C. W. Zacheus, D. A. Agard, and J. W. Sedat, Biophys. J. **94,** 4957 (2008).
14. L. M. Hirvonen, K. Wicker, O. Mandula, and R. Heintzmann, Eur. Biophys. J. **38,** 807 (2009).
15. C. Ventalon and J. Mertz, Opt. Lett. **30,** 3350 (2005).
16. C. Ventalon and J. Mertz, Opt. Express **14,** 7198 (2006).
17. J. Yin, J. Qu, Y. Shao, L. Zhao, H. Lin, and H. Niu, Proc. SPIE **6826,** 682615 (2007).
18. H.-M. Lin, Y.-H. Shao, J.-L. Qu, J. Yin, S.-P. Chen, and H.-B. Niu, Acta Phys. Sin. (in Chinese) **57,** 7641 (2008).